Measurement Science and Technology

100 year anniversary
Measurement Science and Technology

Modelling of electromagnetic wave propagation along transmission lines in inhomogeneous media

To cite this article: C Huebner and K Kupfer 2007 *Meas. Sci. Technol.* **18** 1147

Meas. Sci. Technol. **18** (2007) 1147–1154 doi:10.1088/0957-0233/18/4/023

Modelling of electromagnetic wave propagation along transmission lines in inhomogeneous media

C Huebner[1] **and K Kupfer**[2]

[1] University of Applied Sciences, Mannheim, Germany
[2] MFPA at the Bauhaus-University Weimar, Germany

E-mail: c.huebner@hs-mannheim.de

Received 14 May 2006, in final form 24 July 2006
Published 27 February 2007
Online at stacks.iop.org/MST/18/1147

Abstract
Time domain reflectometry (TDR) is a well-established method for the measurement of moisture in various materials, especially soils. Standard waveform analysis usually provides the average water content along the length of the TDR probe, while more sophisticated methods are required to reconstruct the spatial water content profile. A reconstruction algorithm has been developed which uses one- or two-sided reflection data to calculate capacitance and conductivity distributions from which water content profiles can be derived. Several examples demonstrate the performance of the algorithm under various conditions in lossless and lossy materials.

Keywords: time domain reflectometry with spatial resolution, water content profile reconstruction

1. Introduction

Knowledge of moisture content is essential to many applications in hydrology, agriculture and civil engineering. One of the standard measurement methods is time domain reflectometry (TDR) providing automated moisture monitoring with high accuracy (Robinson *et al* 2005). TDR probes usually consist of two- or three-wire transmission lines which are embedded in the material under test (figure 1). A fast rise time voltage step propagates through the system being partly reflected at the coaxial cable to probe transition and totally reflected at the end of the probe. These reflections show up in the TDR trace from which the wave velocity can be derived. Together with an electrical equivalent circuit of the transmission line and the dielectric characteristics of the material under test the mean water content is calculated.

For many applications this standard waveform analysis is not sufficient. Instead of the mean water content spatial distribution of moisture along the transmission line is required. One approach has been developed by Hook *et al* (1992) dividing the transmission line into several sections by remote-controlled switches. Others change the diameter of the probe to create a series of characteristic reflections or use a number of probes with different lengths (Topp *et al* 1982, Malicki and Skierucha 1989). Besides the coarse local resolution these methods may fail at layered materials with high conductivity. More sophisticated methods consist of modelling the wave propagation along the transmission line in inhomogeneous media and solving the inverse problem in order to retrieve the water content profile (Schlaeger 2005). These methods are usually based on the following electrical equivalent circuit of a very short or infinitesimal piece of the transmission line (figure 2). Each section of the line may have different line parameters according to the water content of the surrounding material. In a lossless material only the capacitance C is influenced by the water content whereas in a lossy material both capacitance C and conductance G are variables.

The transmission line parameters vary with frequency due to the skin effect (R, L) and relaxation of water molecules (C, G) (Heimovaara *et al* 2004). For simplicity the following investigations assume frequency-independent parameters L, C and G. The series resistance R and relaxation processes are neglected. Exemplary relations between the electrical equivalent circuit parameter C, relative dielectric permittivity ε and water content V_W are given by the following equations (see also figures 3 and 4) and are used in the subsequent

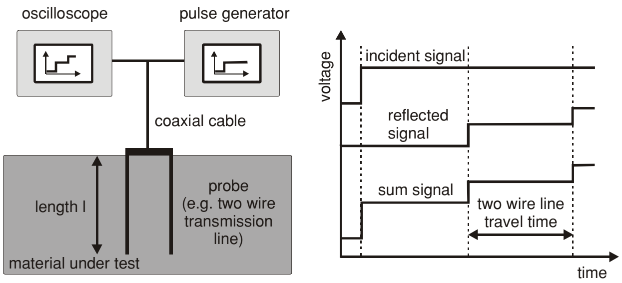

Figure 1. Basic TDR set-up and typical TDR trace (sum signal). Oscilloscope and pulse generator are usually integrated in a single TDR instrument.

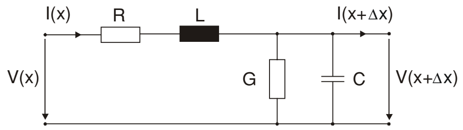

Figure 2. Equivalent circuit of a short section of a transverse electromagnetic (TEM) transmission line. $V(x)$ and $I(x)$ are the voltage and the current at the beginning and end of the section.

simulations:

$$V_W = 1.5789 \times 10^{-5} \cdot \varepsilon^3 - 1.1415 \times 10^{-3} \cdot \varepsilon^2 + 3.765 \times 10^{-2} \cdot \varepsilon - 8.061 \times 10^{-2} \qquad (1)$$

$$C = C_1 + \frac{C_2 \cdot \varepsilon \cdot C_3}{C_3 + \varepsilon \cdot C_4} \qquad (2)$$

with $C_1 = 4.094$ pF m^{-1}, $C_2 = 303.67$ pF m^{-1} and $C_3 = 13.72$ pF m^{-1}. Equation (1) is the inversion of the empirical relation $\varepsilon = f(V_w)$ given by Topp *et al* (1980).

The capacitance of the transmission line depends on its geometry and on the relative dielectric permittivity ε of the surrounding material which is related to the water content (Huebner *et al* 2005). Equation (2) is based on the electrical equivalent circuit of the flat band cable shown in figure 4 which is used in a number of soil moisture measurement applications where sensor lengths up to several metres are required (Kupfer and Trinks 2005).

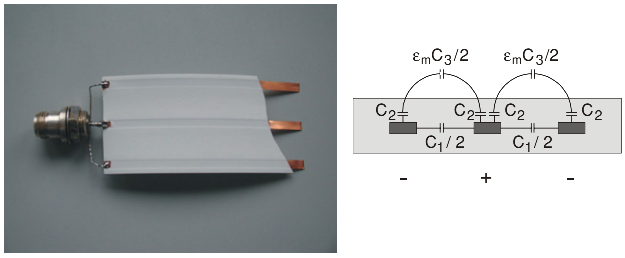

Figure 4. Flat band cable used for TDR measurements and corresponding electrical equivalent circuit.

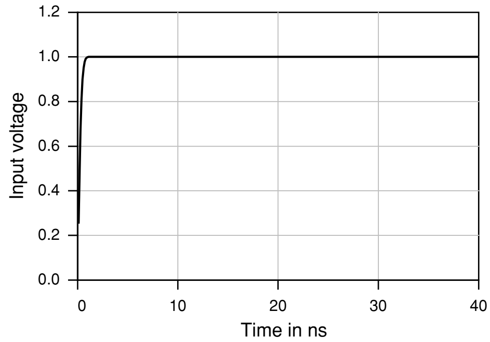

Figure 5. TDR input signal (rise time about 0.5 ns).

2. Step response of inhomogeneous transmission lines

The response of the transmission line to an incident step impulse can be calculated in the time domain (Feng *et al* 1999, Lundstedt and He 1996, Schlaeger 2005) or in the frequency domain (Norgren and He 1996, Heimovaara *et al* 2004). The approach chosen here is to determine the time domain waveforms by the calculation of the scattering parameter $S_{11}(f)$ of a sectioned transmission line in the frequency domain and to perform a subsequent inverse Fourier transform. The algorithm for this so-called forward problem uses an analytical model of the TDR input signal (figure 5):

$$V_{\text{in}} = \text{erf}(\alpha \cdot t) \qquad (3)$$

in which erf is the error function and α is a parameter to adjust the rise time.

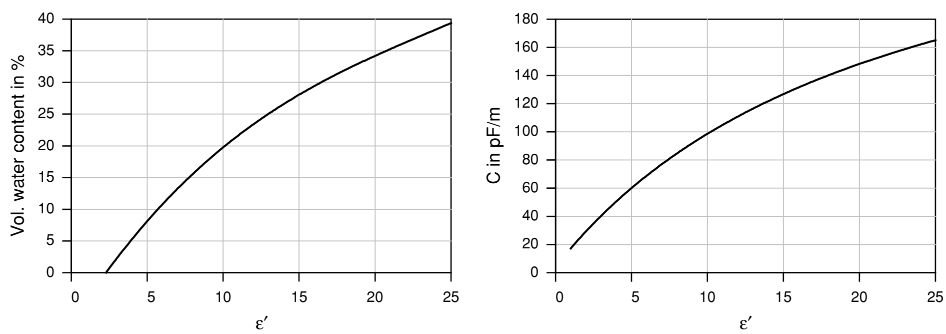

Figure 3. Examples of water content to permittivity (left) and capacitance to permittivity (right) relations.

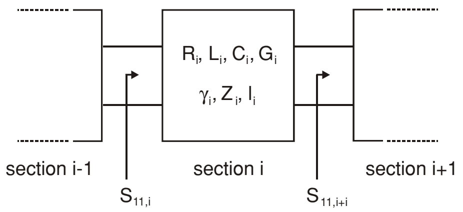

Figure 6. Multisection transmission line.

The reflected signal at the beginning of the multisection transmission line depends on the line parameters $R_i(f)$, $L_i(f)$, $C_i(f)$, $G_i(f)$ of each section and their lengths l_i (figure 6). The algorithm allows for line parameters with arbitrary frequency dependence.

Each section can be described by its propagation coefficient γ_i:

$$\gamma_i = \sqrt{(R_i + \mathrm{j}\omega L_i)(G_i + \mathrm{j}\omega C_i)} \tag{4}$$

and characteristic wave impedance Z_i:

$$Z_i = \sqrt{\frac{R_i + \mathrm{j}\omega L_i}{G_i + \mathrm{j}\omega C_i}}. \tag{5}$$

The following equations relate the reflection factor $S_{11,i+1}$ of the section $i + 1$ to the reflection factor $S_{11,i}$ of section i (Michel 1981):

$$Z_{\mathrm{in},i+1} = \frac{1 + S_{11,i+1}}{1 - S_{11,i+1}} \cdot Z_0 \tag{6}$$

$$\rho_{2,i} = \frac{Z_{\mathrm{in},i+1} - Z_i}{Z_{\mathrm{in},i+1} + Z_i} \tag{7}$$

$$\rho_{1,i} = \frac{Z_i - Z_0}{Z_i + Z_0} \tag{8}$$

$$S_{11,i} = \frac{1}{1 + \rho_{1,i} \cdot \rho_{2,i} \cdot \mathrm{e}^{-2\gamma_i l_i}} \cdot (\rho_{1,i} + \rho_{2,i} \cdot \mathrm{e}^{-2\gamma_i l_i}) \tag{9}$$

Z_0 is the reference impedance, usually 50 Ω. The reflection factor $S_{11,i=0} = S_{11}$ at the beginning of the transmission line is calculated by iterating through all n sections. In case of an open-ended transmission line the iteration starts at the open

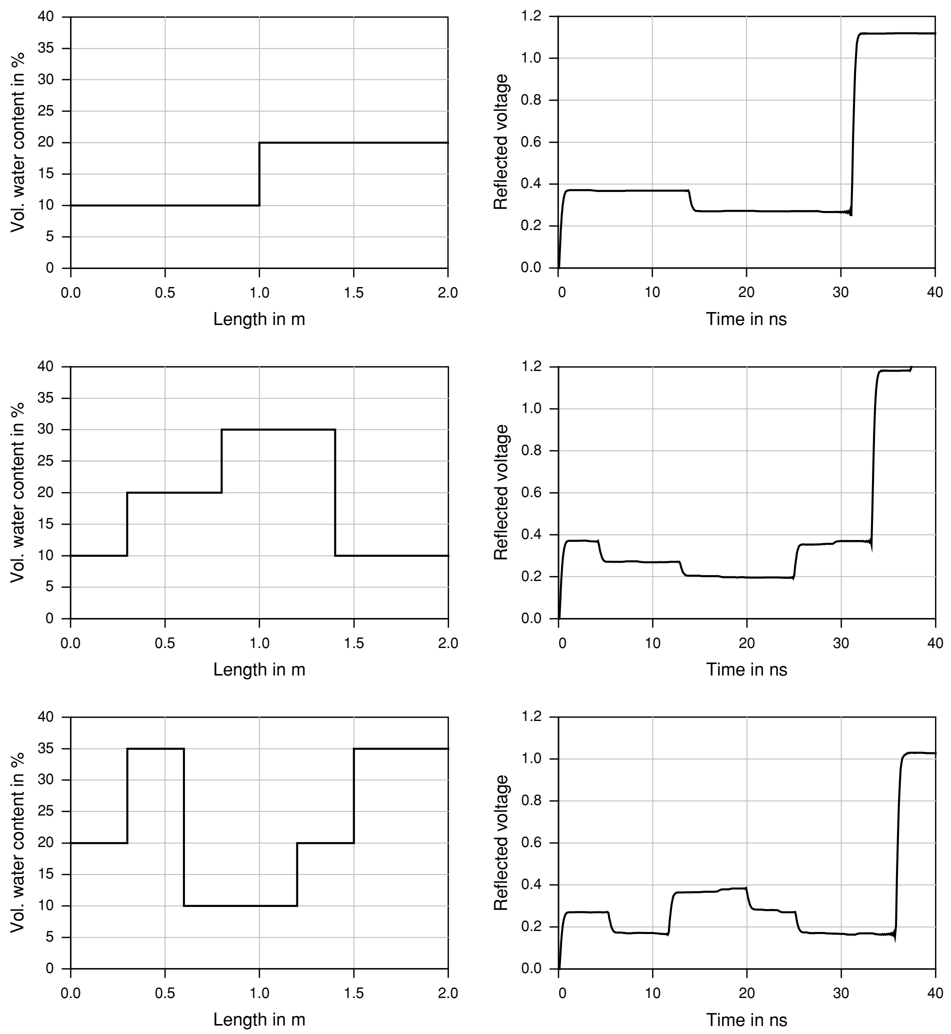

Figure 7. Examples of water content profiles (left) and step response (right) of a 2 m long transmission line embedded in a lossless material.

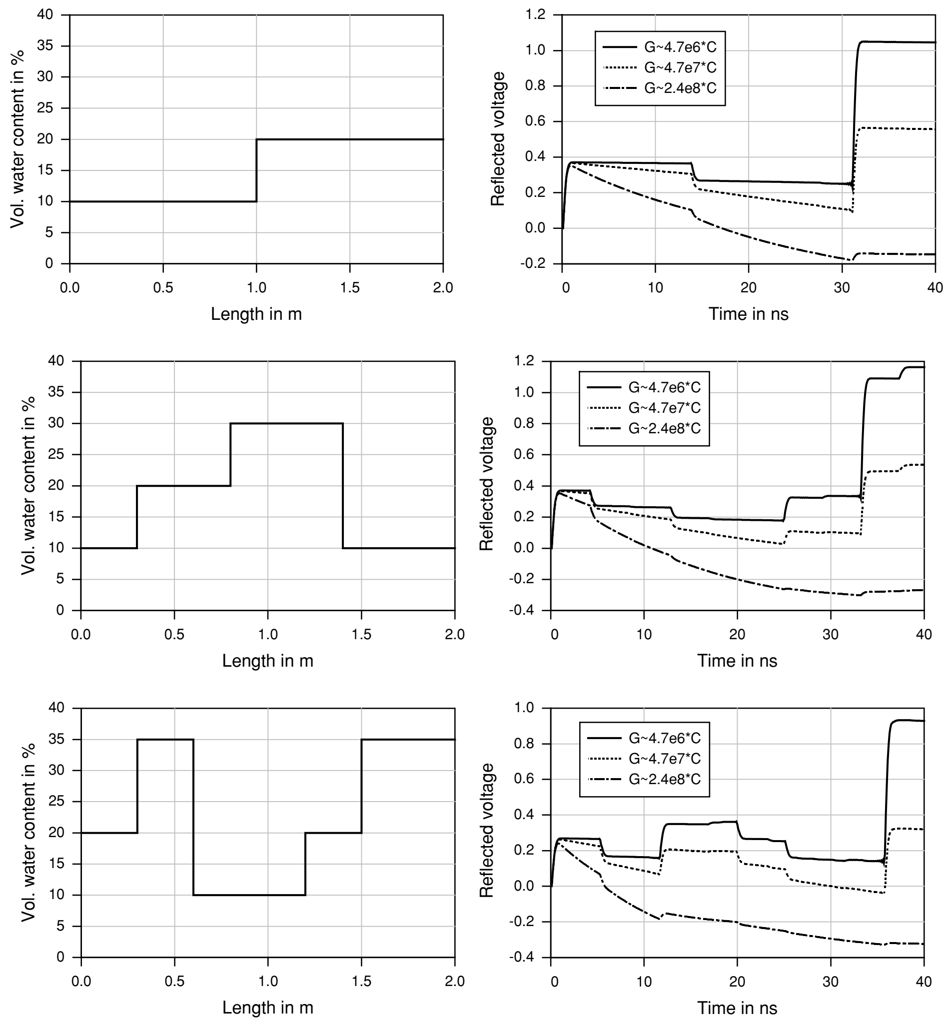

Figure 8. Examples of water content profiles (left) and step response (right) of a 2 m long transmission line embedded in a lossy material.

end of the line with a reflection factor of 1. The dc-value $S_{11}(f = 0)$ depends on the type of transmission line and equals 1 when a dielectric coating around the conductors is used.

The final steps are then to transform S_{11} into the time domain by an inverse Fourier transform:

$$h(t) = \mathit{ifft}(S_{11}(f)) \tag{10}$$

and to convolve the result with the input signal to obtain the reflected signal:

$$V_{\text{ref}} = \text{conv}(V_{\text{in}}, h). \tag{11}$$

Figure 7 shows several examples of water content profiles along a transmission line and the corresponding responses to step-like electrical pulses. Low water content sections are identified by high reflected voltages/fast travel time and vice versa. The strong reflections at around 31 to 36 ns mark the open end of the transmission line. For more complicated and/or continuous profiles the step response is influenced by many multiple reflections. Then more sophisticated methods are required to analyse the waveform and reconstruct the water content profile.

In the case of lossy materials the analysis of the waveform is complicated. The simulations in figure 8 assume that the conductivity is proportional to the capacitance. This is often a reasonable approximation, because losses are mainly due to solute ions in the water fraction. Increasing water content raises capacitance and conductivity at the same time. In the step response the losses reduce the reflected voltage until the partial reflections from the transitions between different water content sections are barely visible. Then, the amplitude resolution of the TDR instruments and noise are limiting factors for any analysis method.

3. Reconstruction algorithm

The reconstruction of transmission line parameters has already been investigated both in time and frequency domains. The methods presented by Lundstedt and He (1996) and Schlaeger *et al* (2001) are computationally fast algorithms in the time domain for frequency-independent line parameters, where the latter is especially suited for automated calculations and batch processing. Frequency domain algorithms are computationally much slower, but easily include frequency-dependent line parameters. In order to account for arbitrary dispersive line parameters a new reconstruction algorithm has been developed which is a combined frequency and

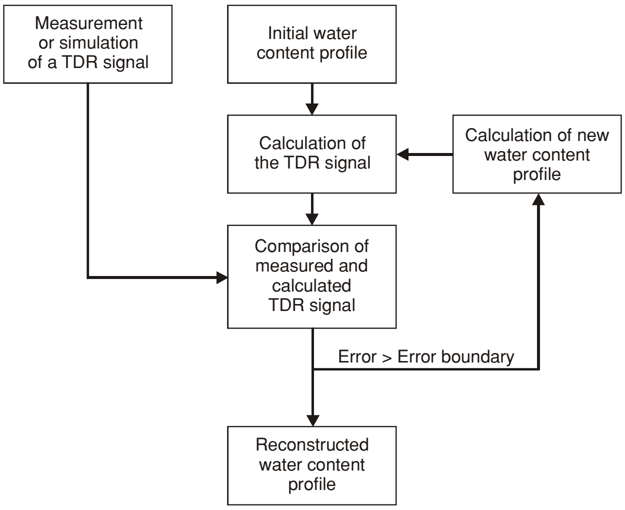

Figure 9. Block diagram of the reconstruction algorithm.

time-domain approach. It is also suited for dielectric-coated transmission lines with enhanced electrical equivalent circuits compared to the simple model shown in figure 2 (Huebner *et al* 2005). Furthermore high frequency models of the coaxial cable to probe transition may be included for a more accurate description of wave propagation. Lundstedt and Norgren (2003) pointed out that it is of crucial importance to estimate the stray capacitance and incorporate it into the calculation.

Figure 9 shows the block diagram of the reconstruction algorithm. The TDR signal (step response) $V_{\mathrm{ref,calculated}}$ is calculated from assumed water content profiles and compared with the measurement $V_{\mathrm{ref,measured}}$. An initial water content profile is iteratively adjusted until a sufficient match between calculated and measured TDR signal is achieved. The objective is to minimize the function $\int_0^{t_{\mathrm{Stop}}} |V_{\mathrm{ref,measured}} - V_{\mathrm{ref,calculated}}|\,\mathrm{d}t$, where t_{Stop} is equal to the round trip time. The convergence criteria depend on the accuracy of the measurement. In case of 8-bit resolution of the TDR instrument the least significant bit corresponds to about 0.4% of the maximum amplitude. So if the differences between $V_{\mathrm{ref,measured}}$ and $V_{\mathrm{ref,calculated}}$ values are less no further refinement will be achieved.

The algorithm has been implemented in Matlab using the optimization toolbox (unconstrained nonlinear optimization). For each iteration the frequency domain response $S_{11}(f)$ is calculated and transformed into the time domain which is computationally slow, but a single transformation of the measured/simulated signal and comparison in the frequency domain has not been successful so far.

The reconstruction algorithm presented in this paper differs from the methods presented earlier by a combination of frequency and time domain calculations. In contrast to the time domain algorithm of Schlaeger (2005) the transmission line parameters are allowed to arbitrarily vary with frequency. Therefore any kind of dispersion may be included in the reconstruction algorithm. The combined frequency and time domain approach requires a Fourier transform for each solution of the forward problem which is computationally slow, but gave the best results with regard to convergence of the optimization.

4. Reconstruction examples

Figure 10 shows an example for a reconstruction of a theoretical water content profile in lossless material ($G = 0$).

The true profile consists of five sections with water contents between 10% and 35%, whereas the initial profile for the reconstruction algorithm is constantly 5%. The corresponding step responses are clearly different at the beginning. After several iterations true and reconstructed signals are getting closer as well as true and reconstructed water content profiles until the algorithm converges.

The three reconstruction results required computation time of 30, 90 and 240 s on a 1.7 GHz mobile Pentium. Each 30 s interval corresponds to five iterations with about 120 function evaluations of the forward problem. Increasing the spatial resolution further improves accuracy (figure 11) at the cost of computation time.

The reconstruction algorithm is well suited for lossy materials if the relation between capacitance and conductivity is known, even in the case of noisy signals. Figure 12 shows a reconstruction example for this case. Capacitance C is assumed to be proportional to conductivity G using

$$G = 0.01S \cdot \frac{C/\mathrm{F} - 40.66 \times 10^{-12}}{165.77 \times 10^{-12} - 40.66 \times 10^{-12}}. \qquad (12)$$

If the relation between the capacitance and conductivity is not known the algorithm has to reconstruct both profiles which doubles the number of unknowns. This is very difficult from one-sided measurements in practical applications. The numerical experiments of Norgren and He (1996) indicated that using only one-sided excitation good simultaneous reconstruction of two parameters (e.g. C and G profiles) with a frequency domain optimization approach could not be obtained. Lundstedt (Lundstedt and He 1996, Lundstedt and Ström 1996) reconstructed two parameters from a one-sided reflection but required data from two times round trip time. In practical applications the resolution and accuracy of the TDR instruments sets limits on the use of the reconstruction algorithm and the number of unknowns to resolve.

From two-sided measurements of the step response it is easier to retrieve both profiles, which can be later transformed into water content again. Figure 13 shows on the left a capacitance and a conductivity profile. The corresponding step responses from the left and from the right side of the transmission line are shown on the right. Both have the same time to the hard reflection at the open end of the line, but the partial reflections are different of course.

The reconstruction results in figure 14 show a sufficient match between true and reconstructed profiles. A finer spatial resolution would give even better results at the cost of computation time.

The disadvantage of two-sided measurements is the requirement for two connections at both ends of the transmission line of course. Therefore standard TDR probes may be replaced, e.g., by flat band cables with attached coaxial feeding lines which require the development of new installation procedures in the field.

Optimization algorithms are usually assessed with regard to their speed of convergence and even more important with

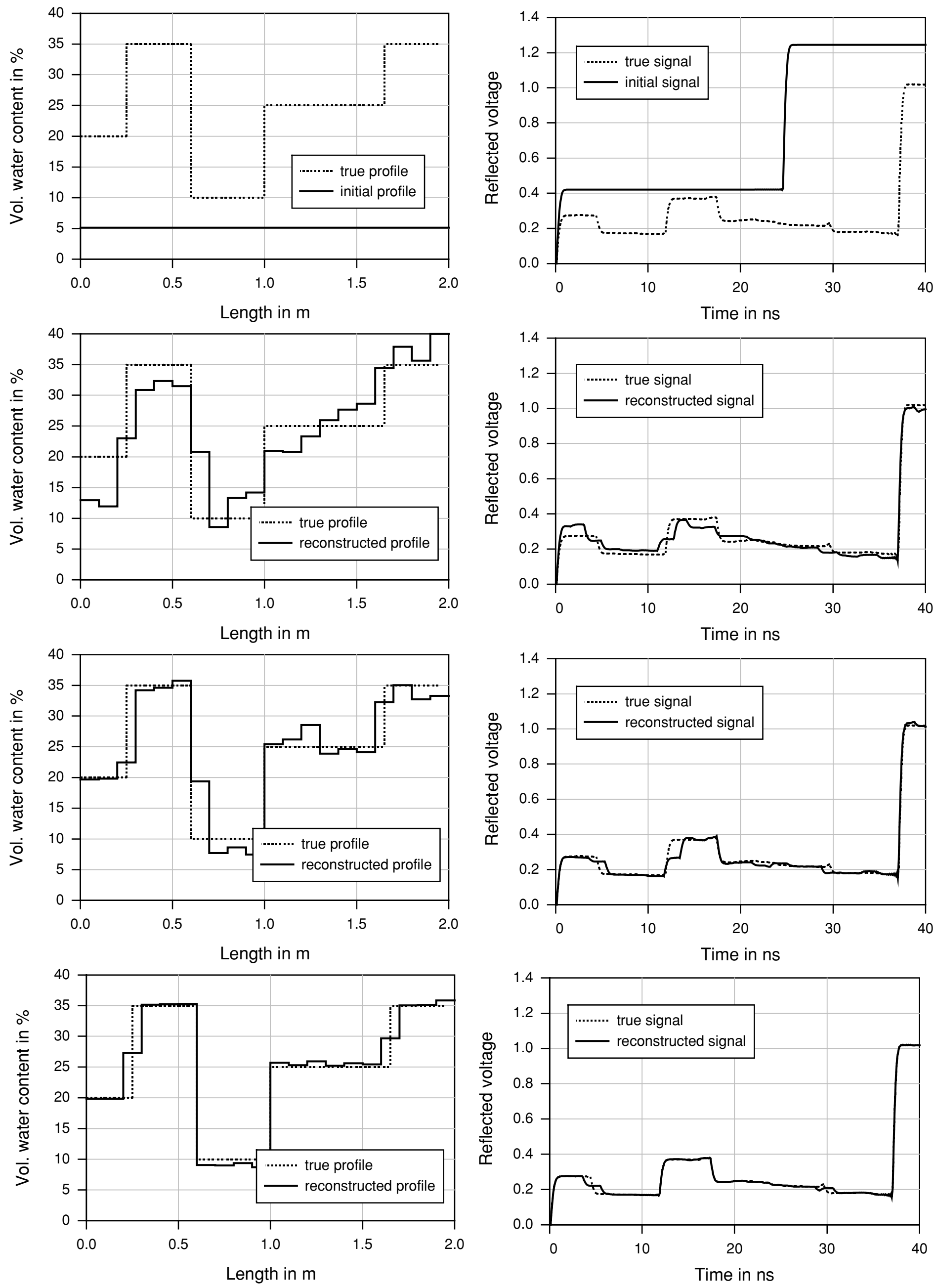

Figure 10. Reconstruction example in lossless material: (left) water content profiles, (right) step response.

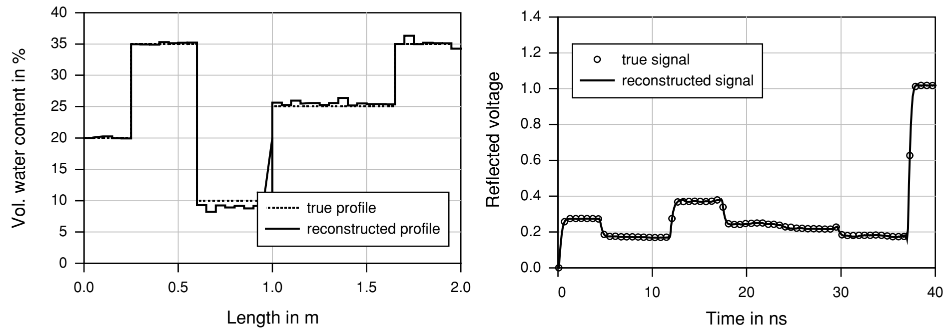

Figure 11. Reconstruction example in lossless material: (left) water content profiles, (right) step response. The spatial resolution is doubled compared to figure 10. The reconstruction required 36 iterations with 1584 computations of the forward problem and took 12.5 min.

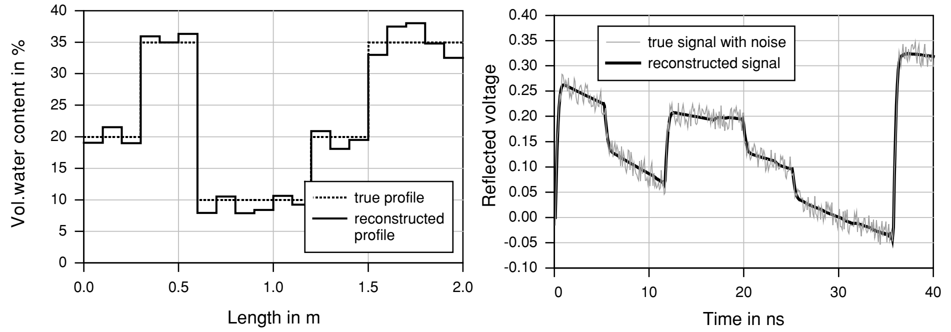

Figure 12. Reconstruction example in a lossy material with noisy step response. Left side: water content profiles, right side: step responses. The noise is low-pass filtered by the algorithm according to the spatial resolution. The reconstruction required 15 iterations with 356 computations of the forward problem and took 14 min.

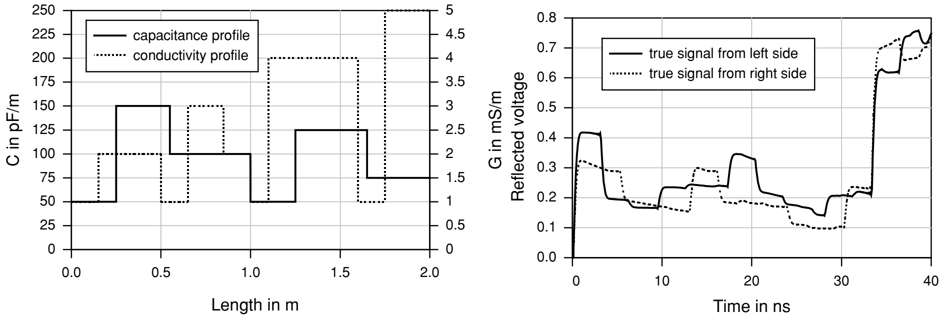

Figure 13. Left: capacitance and conductivity profiles for a 2 m long transmission line embedded in a lossy material, right: step responses from the left and the right ends of the line. The other end is always left open.

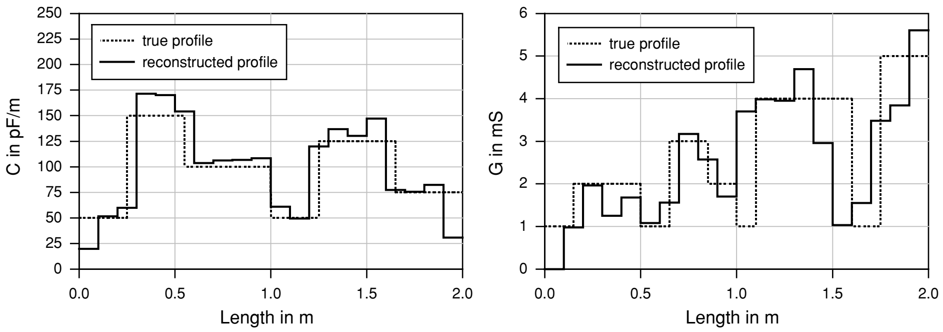

Figure 14. Left: true and reconstructed capacitance profiles, right: true and reconstructed conductivity profiles.

regard to their ability to converge to the right solution (global minimum) and not to stick in a local minimum of the function to be optimized. The reconstruction examples shown in this paper are challenging examples with strong variations of the transmission line parameters. For these worst cases the algorithm always converged to the right solution. A question is about the ability to reconstruct line parameters in the case of dispersion. The examples considered in this study are long transmission lines (2 m) where frequencies up to 1 or 2 GHz are involved and higher frequencies are strongly attenuated. In this frequency range free water relaxation is relatively weak. So conductivity is the main loss mechanism. Further investigations are required to assess the potential of the algorithm in the case of highly dispersive materials where other loss mechanisms like relaxation are becoming more important.

5. Conclusion

Reconstruction of water content profiles is essential for advanced measurement tasks in hydrology, agriculture and civil engineering. A reconstruction algorithm has been developed which is suited both for lossless and lossy materials. It is based on a combined time and frequency domain optimization and accounts for conductive and dispersive materials. Using one-sided measurements capacitance, respectively, water content profiles can be retrieved when the electrical loss mechanism is known. Otherwise two-sided measurements are required for calculating capacitance and conductivity profiles separately. Several simulation examples have shown the performance of the algorithm under various conditions. Practical applications in the field will suffer from the limited amplitude resolution of TDR instruments and noise. Further investigations will be conducted to quantify this influence on the reconstruction accuracy and to study other loss mechanisms than conductivity in detail.

References

Feng W, Lin C P, Deschamps R J and Drnevich V P 1999 Theoretical model of a multisection time domain reflectometry measurement system *Water Resour. Res.* **35** 2321–31

Heimovaara T J, Huisman J A, Vrugt A and Bouten W 2004 Obtaining the spatial distribution of water content along a TDR probe using the SCEM-UA Bayesian inverse modelling scheme *Vadose Zone J.* **3** 1128–45

Hook W R, Livingston N J, Sun Z J and Hook P B 1992 Remote diode shorting improves measurement of soil water by time domain reflectometry *Soil Sci. Soc. Am. J.* **56** 1384–91

Huebner C, Schlaeger S, Becker R, Scheuermann A, Brandelik A, Schaedel W and Schuhmann R 2005 Advanced measurement methods in time domain reflectometry for soil moisture determination *Electromagnetic Aquametry* ed K Kupfer (Berlin: Springer) pp 317–47

Kupfer K and Trinks E 2005 Simulations and experiments for detection of moisture profiles with TDR in a saline environment *Electromagnetic Aquametry* ed K Kupfer (Berlin: Springer) pp 350–65

Lundstedt J and He S 1996 A time-domain optimization technique for the simultaneous reconstruction of the characteristic impedance, resistance and conductance of a transmission line *J. Electromagn. Waves Appl.* **10** 581–602

Lundstedt J and Norgren M 2003 Comparison between frequency domain and time domain methods for parameter reconstruction on nonuniform dispersive transmission lines *Prog. Electromagn. Res.* **43** 1–37

Lundstedt J and Ström S 1996 Simultaneous reconstruction of two parameters from the transient response of a nonuniform LCRG transmission line *J. Electromagn. Waves Appl.* **10** 19–50

Malicki M A and Skierucha W W 1989 A manually controlled TDR soil moisture meter operating with 300 ps rise-time needle pulse *Irrigation Sci.* **10** 153–63

Michel H J 1981 *Zweitor-Analyse mit Leistungswellen* (Stuttgart: Teubner)

Norgren M and He S 1996 An optimization approach to the frequency-domain inverse problem for a nonuniform LCRG transmission line *IEEE Trans. Microw. Theory Tech.* **44** 131–42

Optimization toolbox for Matlab www.mathworks.com

Robinson D A, Jones S B, Wraith J M, Or D and Friedman S P 2005 A review of advances in dielectric and electrical conductivity measurement in soils using time domain reflectometry *Vadose Zone J.* **2** 444–75

Schlaeger S 2005 A fast TDR-inversion technique for the reconstruction of spatial soil moisture content *Hydrol. Earth Syst. Sci.* **9** 481–92

Schlaeger S, Huebner C, Scheuermann A and Gottlieb J 2001 Development and application of TDR inversion algorithms with high spatial resolution for moisture profile determination *Proc. 2nd Int. Symp. and Workshop on Time Domain Reflectometry for Innovative Geotechnical Applications (Evanston, IL, 5–7 September 2001)* pp 236–48

Topp G C, Davis J L and Annan A P 1980 Electromagnetic determination of soil water content: measurements in coaxial transmission lines *Water Resour. Res.* **16** 579–82

Topp G C, Davis J L and Annan A P 1982 Electromagnetic determination of soil water content using TDR: II. Evaluation of installation and configuration of parallel transmission lines *Soil Sci. Soc. Am. J.* **46** 678–84